Journal of the Civil Engineering Forum, May 2022, 8(2):125-138
DOI 10.22146/jcef.3771
Available Online at https://jurnal.ugm.ac.id/jcef/issue/archive

Airfield Asphalt Overlay Design for Non-Conventional Pavement Structures: A Case Study of Airport in Indonesia

Taqia Rahman*, Bambang Suhendro, Hary Christady Hardiyatmo, Wardhani Sartono, Purbolaras Nawangalam
Department of Civil and Environmental Engineering, Universitas Gadjah Mada, Yogyakarta, INDONESIA
Jalan Grafika No 2 Yogyakarta
*Corresponding author: taqia.rahman@ugm.ac.id

SUBMITTED 14 September 2021 **REVISED** 20 November 2021 **ACCEPTED** 25 November 2021

ABSTRACT Airfield pavements gradually deteriorate from several sources, including traffic load and environmental conditions. Consequently, routine maintenance, repair, and rehabilitation should be perfomed to achieve the intended design life. Various studies have examined typical airfield pavements' design and rehabilitation or overlay, mainly focusing on pavements with conventional structures. There is a detailed investigation into airfield asphalt overlay for non-conventional structures, such as a chicken claw or Cakar Ayam pavement and nailed-slab systems. Therefore, this study aimed to examine the challenges and issues for airfield asphalt overlay design for non-conventional pavement structures based on a runway rehabilitation project in one of the major Indonesian airports in 2015. Specifically, the study discussed the overlay design procedure, the evaluation of the existing pavement condition, including visual surveys and deflection tests, and the pre-overlay treatments. A finite element (FE) simulation was developed to model the non-conventional pavement structure to calculate the required overlay thickness. The result showed that data from the falling weight deflectometer (FWD) could not estimate the back-calculated layers' moduli during the overlay design of non-conventional pavement structures. This was because of the difference in the geometric features of the pavement structure. Moreover, the FE model could be a robust tool to simulate the complex three-dimensional geometric features of a non-conventional pavement and important loading conditions. An example of these conditions include the interface shear bond of overlay unavailable in other tools, such as FAARFIELD. Therefore, the additional asphalt overlay could reduce the fatigue stress at the bottom of the existing slab and vertical stress at the top of the subgrade.

KEYWORDS Airfield Pavement, Asphalt Overlay, Pavement Rehabilitation, Overlay Design, Non-conventional Pavement.

1 INTRODUCTION

Airports are valuable assets because they promote regional and worldwide movement of commodities and people. Among the most important infrastructures of an airport is airfield pavement, which provides sufficient load-bearing capacity to ensure safe aircraft operation (Loizos et al., 2017). Airfield pavement gradually deteriorates from several sources during airport operations, such as environmental conditions, aircraft loading, construction issues, and aging (Arabali et al., 2017). Its intended design life is achieved by performing routine maintenance, repair, and rehabilitation. This prevents the pavement from weakening and becoming susceptible to severe distress (Shahin, 2005). The most common form of rehabilitation adopted for airfields is restoration by laying a new pavement layer over the existing structure.

Studies have examined the design of typical airfield asphalt pavements rehabilitation or overlay. Several approaches have been developed worldwide for the overlay design of airfield pavement. An example is the present design approach of the U.S. Federal Aviation Administration (FAA) for airfield pavement (FAARFIELD). It is the most popular tool to calculate the standard thickness of airfield pavement (Gary et al., 2016). However, most existing guidelines and studies are only suitable for pavements with conventional structures.

In Indonesia, several non-conventional pavement structures have been adopted as an alternative to conventional ones, including chicken claw or Cakar Ayam (Suhendro, 2018) and nail-slab systems (Puri, 2018). The two structures are con-

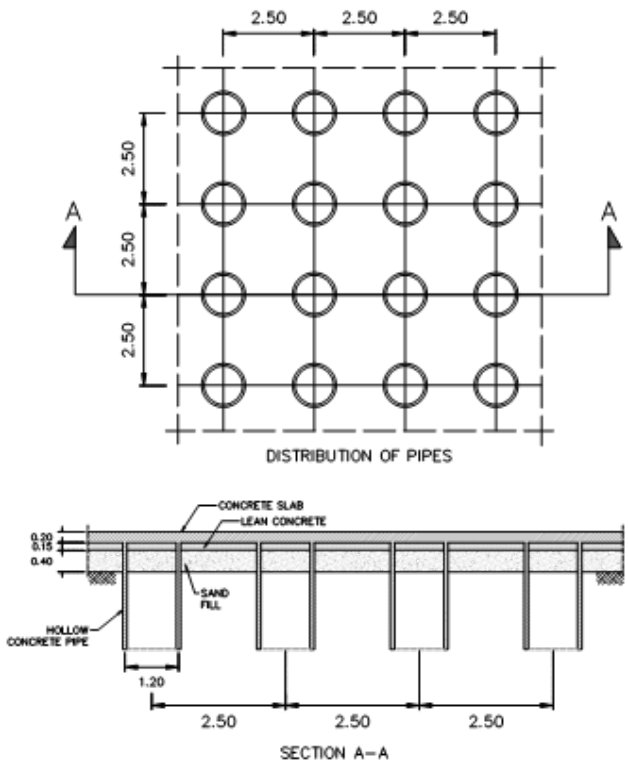

Figure 1 Cross-section drawing of Cakar Ayam pavement system (reproduced from Suhendro (2018)

siderably different from the commonly used conventional pavements. This is because concrete piles or hollow pipes are embedded to the bottom of the reinforced slab or pavement with a particular spacing distance, as shown in Figure 1. The piles or hollow pipes provide significant additional structure stiffness and reduce the deflection and stresses at the bottom of the concrete, especially for projects in areas with soft soil ground (Suhendro, 2018). This non-conventional pavement has been occasionally used for road and airfield pavement application, including Jakarta airport (CGK) and Surabaya airport (SUB), two of the busiest airports in Indonesia. However, there is no detailed investigation into the design procedure and practice of airfield asphalt overlay for non-conventional pavement structures.

This study aimed to examine the challenges and issues for airfield asphalt overlay design for non-conventional pavement structures based on a rehabilitation project in one of the major airports in Indonesia in 2015. It discussed the overlay design evaluation of the existing pavement condition, including visual surveys, deflection tests, and pre-overlay treatments. Furthermore, a finite element (FE) simulation was developed to model the non-conventional pavement structure and calculate the required overlay thickness. These rehabilitation results could help airport authorities and pavement designers make better decisions regarding the airfield asphalt overlay for non-conventional pavement structures in the future.

2 RESEARCH METHODS

2.1 Non-conventional pavement: *CakarAyam*/ chicken claw pavement system

The study airport's runway, taxiway, and apron were constructed using the chicken claw or *CakarAyam* pavement system. It was discovered by Sedyatmo in 1961 and has been widely used for various infrastructures built on relatively soft soil or with low bearing capacity. The *CakarAyam* pavement system comprises a thin, continuously reinforced concrete slab with a thickness of 200 mm. Moreover, the system has concrete hollow pipes embedded to the bottom of the slab with a spacing of 2.5 meters, as shown in Figure 1. The concrete hollow pipe is built with an outer diameter of 1.2 m, a thickness of 80 mm, and a length of 2 m. A low-quality lean concrete layer with a thickness of 150mm and an unbound granular layer of 40 cm thick was laid beneath the concrete slab to provide a uniform base (Suhendro, 2006). The pavement analysis tools commonly used for conventional concrete pavements, such as KENPAVE, BISAR, and FAARFIELD, could not be applied for the *CakarAyam* pavement system due to its unique characteristics. Therefore, an alternative structural analysis method should be developed specifically for the *CakarAyam* system to accurately analyze the influence of the load acting on the top slab on each system component.

2.2 Overlay design procedure

The overlay design procedures are conducted in the order shown in Figure 2. The following section explains each step in detail.

2.2.1 Condition assessment or evaluation of existing pavement

Before the rehabilitation was performed, the existing pavement had experienced several distresses,

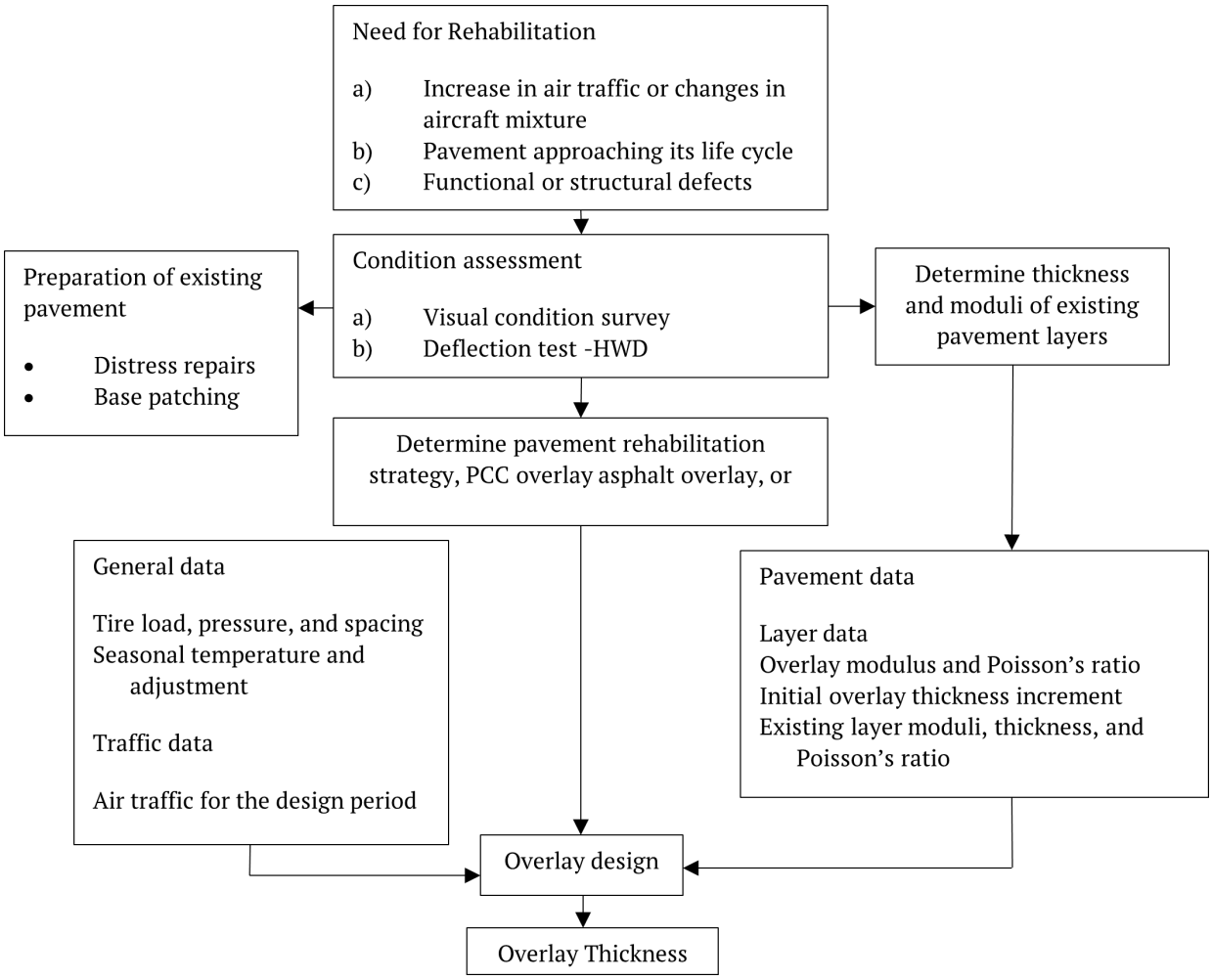

Figure 2 Flow chart of asphalt overlay design

including cracks, punch out, and spalling. The pavement also had old patches caused by the combined effects of traffic loading and the environment over time. Instead of directly performing rehabilitation or asphalt overlay, evaluating the condition of existing pavement and applying the correct treatment could substantially mitigate distress and lengthen the overlay's service life (Zhao et al., 2020). The assessment steps are visual condition surveys, deflection tests, cores, distress recognition, preparation of existing pavement, and repair or base patching.

2.2.2 Visual condition surveys and distress recognition

A visual survey is the most basic and useful survey type (Thom et al., 2013). One commonly used measure of the visual condition is the pavement condition index (PCI), developed by the US Army Corps of Engineers. The approach is based on a summation of the contributions from different distress types such as raveling, cracking, and rutting, and scores on a scale of 100 awarded according to overall condition. In this study, the airport pavement condition index survey was performed following the ASTM D5340 (ASTM, 2012). The first survey was performed for initial pavement condition before any repair. The second survey was performed after pavement repairs, such as crack sealing and patching. The aim was to assess the effect of the pre-overlay repair on improving the pavement condition. The visual survey was a useful method to assess the pavement's health condition and evaluate the correct rehabilitation technique. The crack distress dominated the runway at the study airport and this is expected because the crack is the typical dominant distress for concrete pavement.

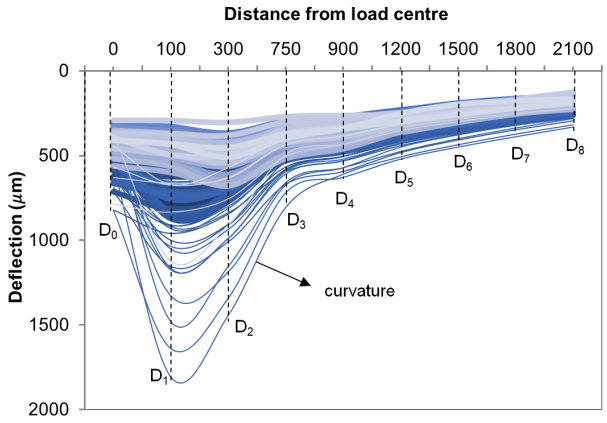

Figure 3 Deflection basin from heavy FWD test at various locations for the runway at the study airport

2.2.3 Deflection tests - Heavy falling weight deflectometer

The falling weight deflectometer (FWD) test is widely used to evaluate pavements' structural condition and predict the layer moduli using the back-calculation process. The test provides sufficient data to evaluate the support of the subgrade, the load transfer condition at pavement joints, and assess the overall structural integrity (Trevino et al., 2003). The FWD involves dropping a specified mass from a predetermined height onto the pavement and measuring the response of dynamic velocity of the pavement surface at various radial points from the applied force (Sørensen and Hayven, 1982). It provides a load to the upper pavement layer comparable to a normal heavy vehicle load pressure (Collop, 2000). This study performed the deflection test using a heavy falling weight deflectometer before and after the pre-overlay repair, similar to the previously discussed visual condition surveys. The maximum load for heavy FWD was set to be 320 kN, with a diameter of loading plate of 300mm, to represent the typical wide-body aircraft that operated in the study airport, such as B777, B747, and A350.

The typical deflection basin in Figure 3 shows that the number of FWD tests with maximum deflection less than 1 mm was 54.5% or 201 from 369 FWD points. Moreover, the proportions of FWD tests with a maximum deflection between 1 mm and 1.5mm and more than 1.5mm were 39.8% and 5.7%, respectively. However, the falling weight deflectometer (FWD) data could not be directly used to estimate the back-calculated layers' moduli. This was due to the difference in the geometric features of non-conventional pavement structures with embedded hollow pipes. It is a major challenge in the asphalt overlay design for non-conventional pavement. Therefore, this study performed other methods to determine the layer moduli, including testing of core samples, Ultrasonic Pulse Velocity (UPV), and hammer test.

2.2.4 Cores, Ultrasonic Pulse Velocity (UPV), and hammer test

This study used more than 15 core samples taken from the runway at the airport. The cores were tested in a laboratory to obtain the compressive and flexural strength of the existing concrete slab. The samples could not be collected for a large quantity due to the core's destructive characteristics. Therefore, ultrasonic pulse velocity (UPV) and hammer tests were performed to investigate the pavement moduli for a wider runway area. The UPV and Hammer test results were calibrated and validated against the data from core samples. The test was useful to obtain the moduli of the existing concrete slab for the analysis.

2.3 Preparation of existing pavement

After obtaining the existing pavement condition, the treatment and repair method is selected. The three procedures commonly used to treat the Portland concrete pavement are base patching, crack break, seating, and rubblization. The approach used was determined by the severity of the pavement's distress (Zhao et al., 2020). This study used base patching and saw-cutting as the most suitable repair method. The crack break, seating, and rubblization methods were not considered because the existing concrete pavement was still in considerably good condition. In this case, cracks occur, but their movement is prevented by steel reinforcement and the hollow concrete pipe.

2.3.1 Design against reflective cracking

Severe distress in the existing concrete pavement should be repaired to ensure it does not reflect through the asphalt overlay. Reflective cracking could develop when cracked or jointed con-

crete layer is overlaid with asphalt (Thom et al., 2013). In rehabilitated pavements, treatment strategies for reflection cracking include using geosynthetic, steel reinforcing mesh, stress absorbing membrane interlayer (SAMI), and double chipping (Dhakal et al., 2016). However, the FAA (2021) does not recommend these technologies in its current regulation. This study ignored the strategy against reflective cracking because the existing concrete pavement is an intact continuously reinforced concrete (CRC) (Thom et al., 2013).

2.4 Selecting the Rehabilitation or Overlay Type

Selecting a rehabilitation method or overlay type of pavement is a crucial decision-making challenge. The materials commonly used for pavement rehabilitation are Asphalt overlay, PCC overlay, comprising bonded concrete with cement grout or epoxy, and Engineered Cementitious Composites (ECC) (Zhao et al., 2020). Asphalt overlays are the most popular methods of Portland concrete pavement rehabilitation (Trevino et al., 2003). ECCs are composites of ultra-ductile fiber-reinforced cementitious, a kind of ductile concrete. Therefore, it could be a suitable overlay material to resist reflective cracking (Ma and Zhang, 2020). This study selected an asphalt overlay to prevent disruptions to airport operation. In this case, the construction could be done during an off-peak period and quickly opened to traffic in several hours (Rahman et al., 2019). The overlay using concrete materials requires seven days to cure before it is trafficked completely. This would not be possible for busy airports such as the study airport.

2.5 Method of Overlay Design or Thickness Calculation

This study performed a three-dimensional finite element (FE) analysis of the chicken claw or $CakarAyam$ pavement system using SAP2000. It is a general-purpose finite element program developed by Computers and Structures Inc. (CSI). In 2004, CSI was used to characterize critical response parameters for the pavement structure with asphalt overlay. These critical responses were used to calculate the thickness of the overlay. This study used a pavement model for analysis, an updated version from the previous model developed by Rahman et al. (2015). Numerous changes have been made to improve the accuracy of simulations, including the use of solid elements instead of shell elements.

2.5.1 Description of model development

Figure 4 shows the pavement structure simulating the $CakarAyam$ pavement system. Layer thicknesses are obtained from the construction documentation drawing and based on the cores taken from the field. Table 1 presents the length and width of the model and loaded area. The model size of 10 m x 10 m was sufficiently far from the load and did not affect the model's edge. This study varied the overlay thickness from 100 m to 200 m with a thickness increment of 10 mm for simulation purposes. Furthermore, no degrees of freedom were restrained in the horizontal direction for the boundary condition. However, translation in the three principal directions was prevented at the bottom of the subgrade. Figure 4 shows that the model was subjected to B777 landing gear in the full six-wheel bogie to anticipate the effect of the wheel configuration of the dual-

Table 1. Dimension of the pavement model

Component	Dimension				
	Length	Width	Thickness	Diameter	Pipes spacing
Asphalt overlay	10 m	10 m	varied*	-	-
Hollow concrete pipe	2 m	-	0.08 m	1.2 m	2.5 m
Existing concrete slab	10 m	10 m	0.2 m	-	-
Lean concrete	10 m	10 m	0.25 m	-	-
Granular sub-base	10 m	10 m	0.4 m	-	-
Subgrade	10 m	10 m	2 m	-	-

*Initial overlay thickness: 100 mm, thickness increment: 10 mm

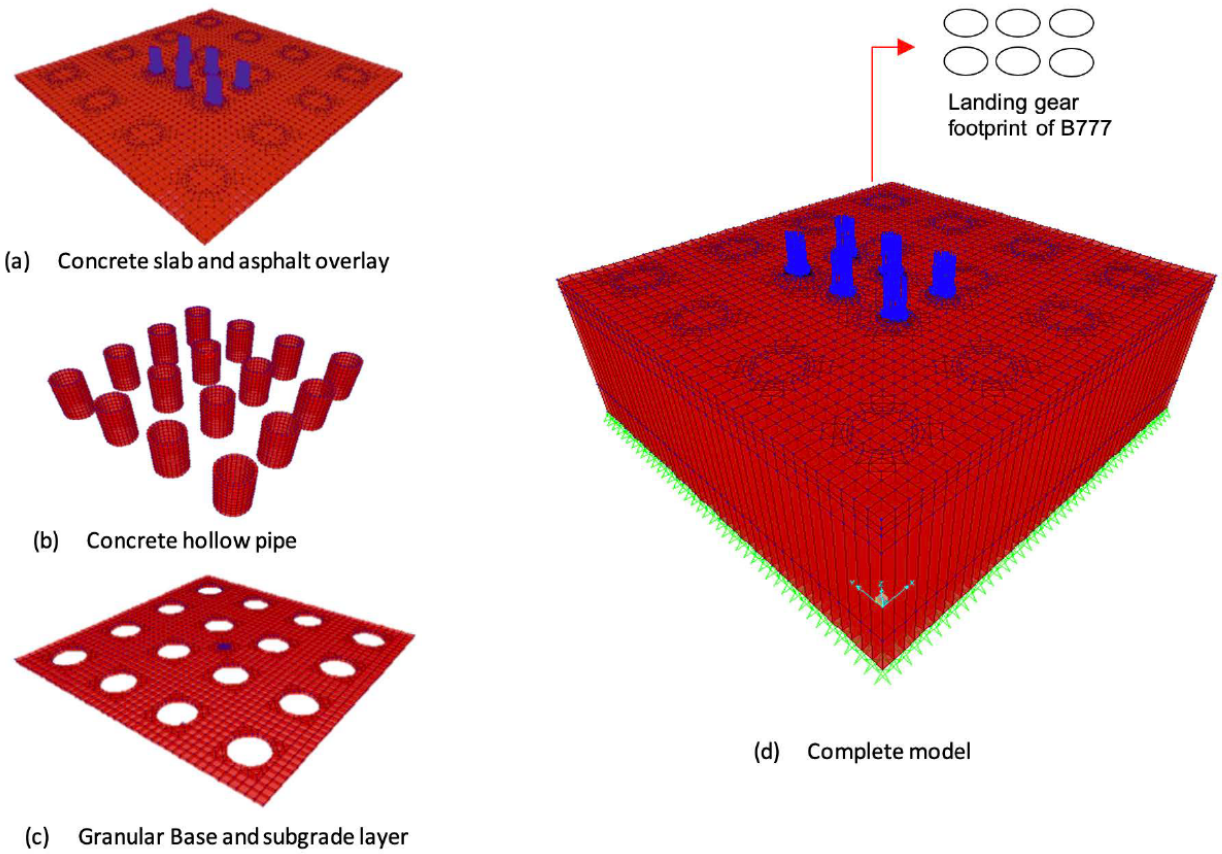

Figure 4 3D view of FE model for a six-wheel dual-tridem landing gear (B777) configuration

Table 2. Dimension of the pavement model

Layer	Poisson's ratio 0.35	Modulus (MPa) varied*
Existing concrete slab	0.15	23,452
Hollow concrete pipe	0.15	23,452
Lean concrete	0.20	2,300
Granular sub-base	0.35	150
Subgrade	0.35	66

tridem of B777 on the pavement. The tire loading characteristics follow the specifications from the airplane manual for a Boeing 777-300ER (Airplanes, 2015). The B777 aircraft was selected for analysis because it is one of the most frequent aircraft operated in the study airport, with 13,450 annual departures in 2013. Moreover, it provided the highest aircraft classification number (ACN) on rigid pavement, making it the most critical aircraft. The typical take-off weight of a single wheel load of 262.35 kN was considered, and tire pressure of 1.52 MPa, giving a contact area of 1752 cm^2, was applied. The tire footprint area was assumed to be 1.6 ellipses, as suggested by Boeing (2017), with major and minor axes of 0.59 m and 0.37 m, respectively. This model's validity has been verified using HWD (31 tonnes) data and a B-747 bogie full-scale test load performed by Aeroport De Paris, 1983 (Rahman et al., 2015). The validation results showed a good agreement between model output and measured pavement deflections.

2.5.2 General input data

Table 2 shows the pavement characteristics, including the subgrade soil and the granular base

moduli, lean concrete, and concrete slab determined and calibrated from validated HWD FE model, core drill, UPV, and Hammer test. These layer characteristics were used for the analysis. The asphalt overlay properties were simplified by assuming a single modulus value obtained following the FAARFIELD as a function of temperature calculated using Witczak (1989) equation:

$$log_{10}(E_{AC}) = 1.53657 - 0.006447 \times T - 0.00007404 \times T^2 \quad (1)$$

where E_{AC} is the modulus of asphalt (105 psi), and T is the temperature of asphalt concrete (°F). The design asphalt temperature was assumed to be 32°C (89.6 °C). Based on this formula, the modulus value of 1,400 MPa was obtained for this temperature. Additionally, the modulus corresponding to higher (60°C) and lower temperatures (15°C) was used to verify the overlay design in the thermal stress analysis, as discussed in section 3.4.

Other significant airplanes in the traffic mix must be converted to a design airplane's gear type and load magnitude to complete the equivalent traffic calculation into a single design aircraft. Boeing 777-300ER was selected as the design aircraft for this study, while the conversion process was conducted according to the old standard of FAA: AC 150/5335-5A (FAA, 2006). The following is a summary of the general assumptions used for the overlay design:

- Pavement data
  Existing concrete slab compressive strength: 25.3 MPa
  Modulus of subgrade reaction: 40-45 MN/m^3
  Existing concrete slab flexural strength: 3.77 MPa
- Traffic data
  Design aircraft: B777-300ER
  Design period: 20 years
  Traffic: 120,000 coverages
  Maximum take-off weight: 351.535 kg

2.6 Design of interlayer shear bond strength

Airside pavements encounter routine aircraft movement activities, such as taxiing, take-off, deceleration during landing, and rapid turning in exit taxiways (Wang et al., 2016). These movements could produce high shear stresses at the surface and interface of pavement (Mohammad et al., 2012). The premature interlayer shear failures that occurred after asphalt overlay operation during hot weather were recorded in Indonesian airports during 2017 and 2019, as shown in Figure

(a) Lampung (TKG) airport, May 2017

(b) Yogyakarta (JOG) airport, November 2019

(c) Halim Perdana Kusuma Jakarta (HLP) airport, July 2017

Figure 5 Interface shear failure of newly laid asphalt overlay (sources: Indonesian Airport Authority and Ministry of Transportation Republic of Indonesia)

5. These accidents have caused extensive, costly airport closures and flight delays. The guideline on pavement overlays by FAA focuses only on thickness determination. They do not provide directions on interlayer shear bond strength design that could resist aircraft barking and turning movement. Therefore, this study investigated the effect of aircraft braking movement on the interlayer between asphalt overlay and concrete.

This study investigated the steady braking of aircraft during landing and full braking conditions. Data regarding the full braking operation (FB) of B777 aircraft was obtained from the airplane manual issued by Boeing. Furthermore, the shear force was assumed to be equal to the normal or vertical load multiplied by a coefficient of tire-pavement friction of 0.8 for dry surface conditions shown in Equation 3. Steady breaking was assumed for the landing operations, and the vertical landing load was obtained from the airplane manual. Moreover, the shear force during the full braking operation was adopted from White (2016), equal to the aircraft mass multiplied by the rate of airplane deceleration, as shown by Equation 2. Therefore, a landing deceleration of 3.0 m/s^2 (O'Massey, 1978) was adopted.

$$F_{SB} = \frac{m \times d}{1000} \tag{2}$$

$$F_{FB} = N \times \mu \tag{3}$$

where F_{SB} is the steady braking force during landing operation (kN), F_{FB} is the longitudinal or braking force during full braking operation (FB) (kN), N is the vertical load (kN), μ is the coefficient of friction of the tire-pavement contact (0.8 in this case), m is the mass of the aircraft acting on a single wheel (kg), and d is the rate of airplane deceleration during landing (m/s^2). The estimated forces at the critical points for steady and full braking of a B777 aircraft are 209.9kN and 80.3kN, respectively.

3 RESULT AND DISCUSSION

3.1 Asphalt Overlay Design

The FAA design procedure considers the Cumulative Damage Factor (CDF) to replace the design airplane concept. In the CDF concept, the contribution of each aircraft in a certain mix of traffic is computed to acquire the cumulative damage from all aircraft operations (FAA, 2021). The damaging effects of each aircraft in the traffic mix were calculated based on gear spacing, gear location, and load. For flexible pavement, the CDF corresponds to the tensile and rutting failures at the bottom of the asphalt layer and on top of the subgrade, respectively. In contrast, it corresponds to the failure at the bottom of the concrete slab for rigid pavement. However, the CDF concept could not be applied for the developed FE model in this study of non-conventional pavement structures. This is because it would be extremely expensive and time-consuming to design the model for each

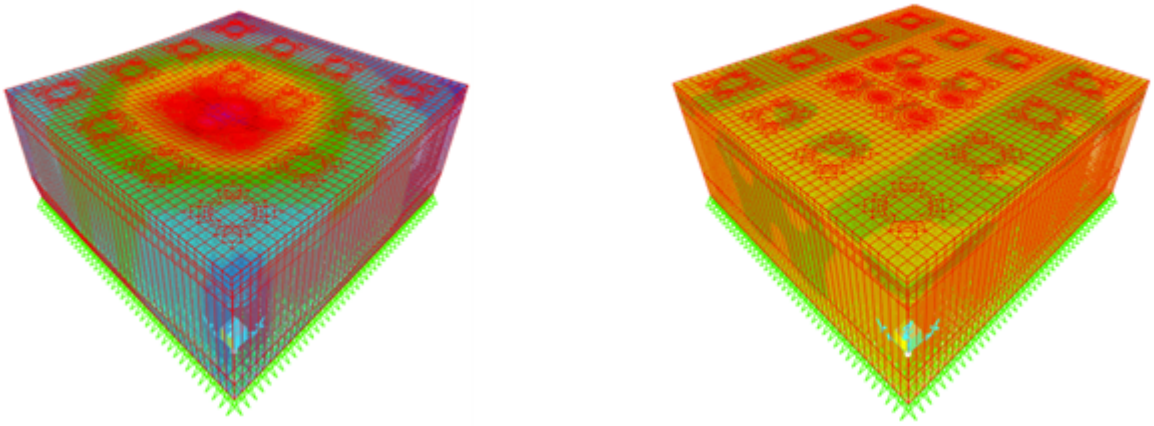

(a) Deflection (in mm)

(b) Horizontal stress (MPa)

Figure 6 The results of the model: deflection and horizontal stresses for structure with 190-mm-asphalt overlay

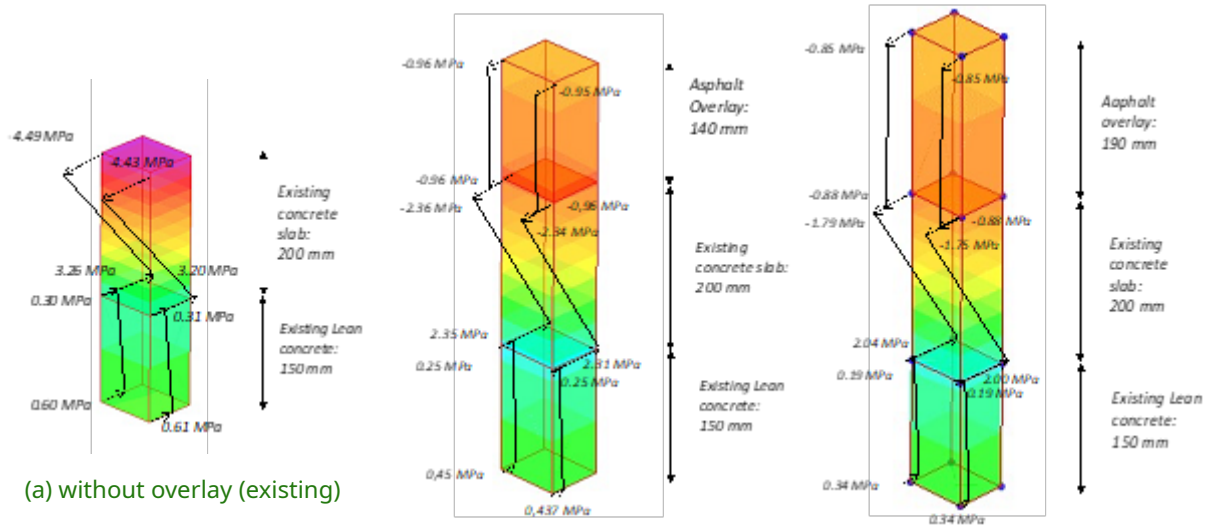

(a) without overlay (existing)

(b) 140-mm-asphalt overlay

(c) 190-mm-asphalt overlay

Figure 7 Illustration of horizontal stress on the asphalt overlay and the existing concrete slab and lean concrete under vertical load

aircraft operating at the airport. The old concept of equivalent departures of a single-designed aircraft would be the realistic technique, as discussed in sub-section 2.6.2. The model results in Figure 6 show the deflection and horizontal stresses. An explanation of the overlay thickness calculation is provided in the following section.

3.2 Stress within the pavement

The overlay design procedure is primarily established based on horizontal tensile strain at the bottom of the overlay, horizontal stress at the bottom of the PCC slab surface, and vertical strain at the top of the subgrade. Figure 7 shows the graphs from the analysis results, containing stresses within the pavement elements for overlay thickness of 140 mm and 190 mm asphalt and the existing layer without an overlay. Compared to the existing layer without overlay, adding thick asphalt overlays significantly reduced the horizontal stresses at the bottom of the slab layer. The stresses were reduced from 3.26 MPa to 2.35 and 2.04 for asphalt overlay of 140 mm and 190 mm, respectively. This suggests that the asphalt concrete overlay increases the structural capacity of the existing pavement, extending its expected life. Table 3 shows the maximum stresses within the pavement for an asphalt overlay of 190 mm.

3.3 Pavement overlay thickness design

The required overlay thickness should give acceptable damage levels under a specified traffic condition. The damage levels are determined by fatigue cracking at the bottom of the asphalt overlay and existing concrete slab and rutting at the top of the subgrade. These criteria are commonly used for mechanistic analysis-based overlay design (Pierce and Mahoney, 1996). This study used the FAAFIELD model for the rutting failure of the subgrade defined as follows (Brill and Kawa, 2017):

for C > 1000 coverages,

$$log_{10}(C) = (-0.1638 + 185.19\varepsilon_v)^{-0.60586} \quad (4)$$

for C ⩽ 1000 coverages,

$$C = \left(\frac{0.004141}{\varepsilon_v}\right)^{8.1} \quad (5)$$

where C is the coverage level, and ε_v is the vertical strain at the top of the subgrade. The fatigue cracking failure model for several allowable repetitions for the asphalt overlay was calculated following the Heukelom and Klomp failure model adopted in FAARFIELD (Loizos et al., 2017):

$$\begin{aligned}\log_{10}(C) =& 2.68 - 5\times \log_{10}(\varepsilon_h) \\ & - 2.665\times \log_{10}(E_{AC})\end{aligned} \quad (6)$$

where ε_h is the horizontal tensile strain at the bottom of the asphalt layer and E_{AC} is the elastic modulus of the asphalt layer (psi). The rigid pavement failure model uses the design factor DF, the ratio of flexural strength R of concrete to calculated horizontal stress on the bottom of the concrete slab,). It is linear in the logarithm of C (Brill and Kawa, 2017):

$$DF = \left[\frac{bd}{0.8b + 0.2d}\right] \times \log C + \left[\frac{0.8bc + 0.2ad}{0.8b + 0.2d}\right] \quad (7)$$

$$\begin{aligned} b &= d = 0.16 \\ a &= 0.760 + 2.543{\times}10^{-5}\,(E - 4500) \\ c &= 0.857 + 2.314{\times}10^{-5}\,(E - 4500) \end{aligned} \quad (8)$$

where a, b, c, and d are fitting parameters obtained from full-scale tests by FAA and E is the design subgrade modulus in psi. Using the formula and the stress and strain-state obtained from the analysis in Table 3, the results of the overlay thickness determination indicate that 190mm was the overlay thickness required for this project.

3.4 Checking for the thermal stress

Concrete pavement is sensitive to the changing ambient temperature that could easily cause cracking. This study performed the thermal stress analysis using the same model as the previous analysis to consider the effects of pavement temperature on structural parameters. The analysis was based on the assumption of two extreme conditions of sunny daytime and nighttime.

Figure 8 shows the temperature distribution on the asphalt overlay, concrete slab, and underlying layers for the two conditions. Table 4 shows the thermophysical properties of pavement materials adopted in this study.

The calculation results in Figure 9b show that the thermal stress caused the curling stress on the pavement. Although curling stress was not as significant as traffic-induced stresses, it increased cracking potential and reduced pavement life (Setiawan, 2020).

Therefore, it is important to consider the thermal stress caused by temperature distribution in

Table 3. Maximum horizontal, shear, and compressive stresses and strains for overlay thickness of 190mm

Location	Maximum stresses and strains for overlay thickness of 190mm:			
	Horizontal stress (S11/S22), MPa	Compressive stress (S33), MPa	Horizontal strain (11/ 22), microstrain	Compressive strain (33), microstrain
Overlay (top)	-1.11	-1.47	-244	-564
Overlay (bottom)	-1.01	-1.47	-159	-524
Existing concrete slab (top)	-2.20	-1.78	-94	-90
Existing concrete slab (bottom)	2.12	-1.78	160	-66
Subgrade (top)	0.025	-0.014	625	-392

Table 4. Thermo-physical properties of pavement

Component	Properties				
	Thickness	Density (kg/m^3)	Specific heat (J/kg/K)	Thermal conductivity (W/m/k)	Coefficient of thermal expansion $(°C)^{-1}$
Asphalt overlay	varied*	2400	800	1.89	$40 .10^{-6}$
Hollow concrete pipe	0.08 m	2400	880	1.70	$9.9 .10^{-6}$
Existing concrete slab	0.20 m	2400	880	1.70	$9.9 .10^{-6}$
Lean concrete	0.25 m	2200	840	1.55	$7.2 .10^{-6}$
Granular sub-base	0.40 m	2100	805	1.13	$11.25 .10^{-6}$
Subgrade	2.00 m	1900	1100	1.10	$18 .10^{-6}$

*Initial overlay thickness: 100mm, thickness increment: 10mm

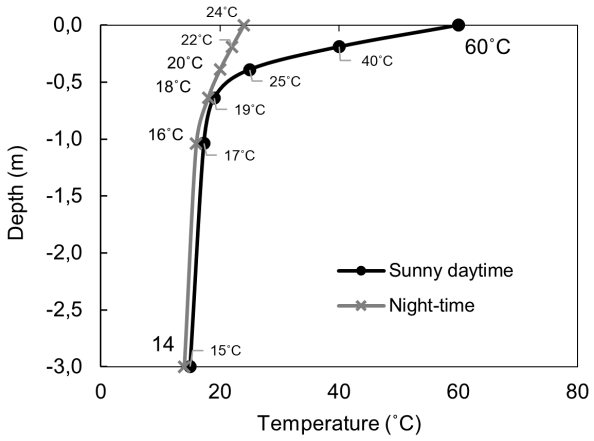

Figure 8 Temperature distributions throughout the slab depths on sunny daytime and nighttime

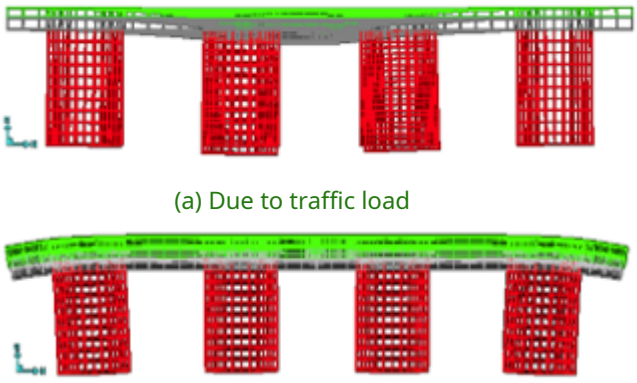

(a) Due to traffic load

(b) Due to thermal stress

Figure 9 Deflection of the pavement

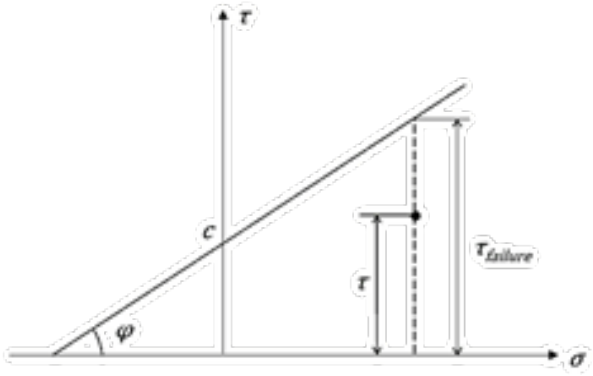

Figure 10 Representation of the Mohr-Coulomb failure criterion (reproduced from Wang et al., 2016)

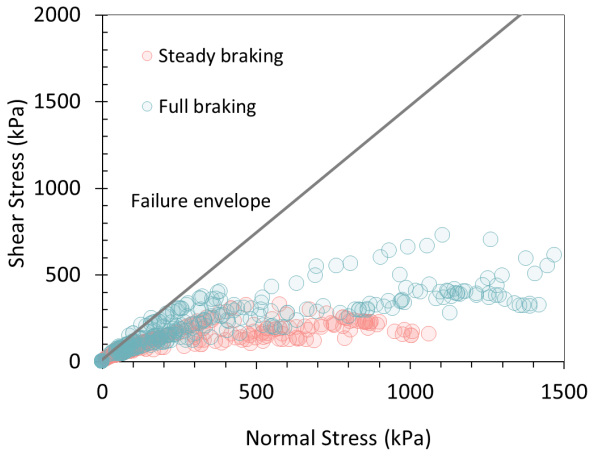

Figure 11 Critical stress at interface under steady and full braking of B777 aircraft

the structural analysis of airport pavements. The overlay thickness of 190 mm selected in this study was sufficient to resist traffic and thermal load.

3.5 Checking the interlayer shear bond strength

The analysis of the interlayer shear bond strength between the concrete slab and overlay was performed using the assumption described in section 2.7. The aim was to investigate the potential interface shear failure or delamination of asphalt overlay. Furthermore, the Mohr-Coulomb criteria in Figure 10 (Mohammad et al., 2012) was used to investigate the susceptibility of the asphalt overlay interface to shear failure. The technique has been frequently utilized to estimate pavement interface shear failure (Wang et al., 2016). The Mohr-Coulomb theory suggests that interface failure is controlled by normal and interface shear stress. The linear Mohr-Coulomb envelope for interface shear strength is shown in Equation 9 (Wang et al., 2016):

$$\tau_{failure} = c + \sigma tan\ \phi \quad (9)$$

where $\tau_{failure}$ is shear stress at failure (kPa), c is cohesion (kPa), σ is normal stress (kPa), and ϕ is the angle of internal friction in degrees.

In this study, the cohesion (c) was approximated to be 12.2 kPa with an angle of internal friction (ϕ) of 55.7° for PCC-asphalt interlayer with a typical cationic tack coat at 60°C (Rahman et al., 2020). A stress-to-strength ratio was defined using Equation 10 (White, 2016) to assess the criticality of traffic-imposed stresses at the interface. A higher ratio closer to 1 implies a higher possibility of shear failure.

$$\text{Stress-to-strength Ratio} = \frac{\tau_c}{\tau_{failure}} = \frac{\tau_c}{c + \sigma tan\alpha} \quad (10)$$

where τ_c is calculated shear stress (kPa).

The stress state points from the FE model were examined against the failure envelopes to determine the criticality of the shear stress at the asphalt overlay interface. Figure 11 shows the shear stress states for steady braking (SB) and full braking (FB) movement of B777 aircraft for 190mm-asphalt overlay. The failure envelope is displayed with the stress states to examine the shear failure potential of the layer interface. The maximum stress-to-strength ratio under various aircraft movements was 0.96 and 0.81 for FB and SB loading, respectively. A high stress-to-strength ratio demonstrates the susceptibility of the asphalt overlay interface to shear bond failure.

This result indicates that the aircraft braking movement was slightly under the failure envelope. In this case, the interface could still resist the forces applied for the selected asphalt overlay thickness. Therefore, the interface shear bond analysis is essential in assessing the potential shear failure of the newly laid asphalt overlay.

4 DISCUSSION

This study discussed the design process of airfield asphalt overlay of non-conventional pavement structures. It presented the overlay design procedure evaluation of the existing pavement condition, including visual surveys and deflection tests, pre-overlay treatments, and thickness calculation using FE. The results showed that evaluating the existing pavement health is an important process before the overlay was performed. Moreover, visual surveys and non-destructive deflection tests and cores could be valuable tools for assessing pavement structure and estimating pavement moduli (stiffness). It is important to classify the pavement as jointed or continuously reinforced concrete to select the correct evaluation technique for non-conventional pavement structures, such as $CakarAyam$ pavement. The right diagnosis and treatment would prevent the failures and crack from reflecting through the new asphalt overlay. The data from the deflection test using a falling weight deflectometer (FWD) could be used for back-calculation to estimate the layer stiffness (moduli) for typical pavement structures. However, this is not the case for the non-conventional pavement structure with piles or concrete hollow pipes beneath the pavement layer. FWD test could still assess the existing pavement health and validate the developed finite element model. This is probably the main challenge of the overlay design of non-conventional pavement structures.

The other important issue is the selection of the rehabilitation technique. This study selected the asphalt overlay during the nighttime period because the airport returned to service each morning. The approach could keep the minimal impact on the airport's closure and reduce the interruption to the airport services. This is because the study was conducted on a busy airport that could not be closed for a prolonged period. However, it is necessary to consider construction management, safe workplace, and proper quality control to improve pavement quality during nighttime construction (Zhao et al., 2020). It is essential to provide a tapered joint to transition between the new asphalt layer and existing pavement. Additionally, the lighting system and line marking should be returned to their original conditions in every work period.

The calculation of the required thickness for the overlay design of the non-conventional pavement structure could not be analyzed using well-established computer programs such as FAARFIELD, KENPAVE, and BISAR. This is due to the difference in the geometric features of the pavement structure. Therefore, the finite element (FE) model could simulate the complex three-dimensional geometric features of a non-conventional pavement structure. FEM evaluates several important loading conditions and input features. These include interface shear bond strength conditions and the effect of thermal load or curling stress usually ignored in FAARFIELD and other techniques. The evaluation of interface shear bond condition prevents premature failure, and the delamination frequently observed in newly laid asphalt overlay in several airports in Indonesia. Adding a thick asphalt concrete overlay reduces the fatigue stress at the bottom of the existing slab and vertical stress at the top of the subgrade. Therefore, it increases the structural capacity of the existing pavement and extends the expected pavement life.

5 CONCLUSIONS

This study aimed to examine the challenges and issues for airfield asphalt overlay design for non-conventional pavement structures. The examination was based on an actual rehabilitation project in one of the major airports in Indonesia in 2015. The following conclusions were drawn:

1. Evaluation of existing pavement condition and pre-overlay treatment and repairs are essential in preventing the failures and cracks to reflect through the new asphalt overlay.
2. The data from the deflection test using the falling weight deflectometer (FWD) could not be used to estimate the back-calculated layer stiffness (moduli) for the overlay design of non-conventional pavement structures. This is due to the difference in the geometric features of the pavement structure. However, the FWD test could still be useful to validate the developed pavement model.
3. The finite element (FE) model could simulate the complex three-dimensional geometric features of a non-conventional pavement structure.
4. The FE model evaluates several important loading conditions and input features. These include interface shear bond strength conditions and the effect of thermal load usually ignored in FAARFIELD and other techniques.
5. The FAA's new concept of Cumulative Damage Factor (CDF) calculates the effect of each aircraft in the traffic mix on the pavement. However, it is not feasible to be applied for the developed FE model of the non-conventional pavement structure because it would be extremely expensive and time-consuming. Therefore, the concept of equivalent departures of a single design aircraft would be the realistic technique.
6. Adding a thick asphalt concrete overlay increases the structural capacity of the existing pavement, extending the expected pavement life.

DISCLAIMER

The authors declare no conflict of interest.

AVAILABILITY OF DATA AND MATERIALS

All data are available from the author.

ACKNOWLEDGMENTS

The authors are grateful to PT. Angkasa Pura II for supporting this study.

REFERENCES

Airplanes, B. C. (2015), '777-200lr/-300er/-freighter airplane characteristics for airport planning, document number d6-58329-2', *URL http://www. boeing. com/assets/pdf/commercial/airports/acaps/777_2lr3er. pdf* .

Arabali, P., Sakhaeifar, M. S., Freeman, T. J., Wilson, B. T. and Borowiec, J. D. (2017), 'Decision-making guideline for preservation of flexible pavements in general aviation airport management', *Journal of Transportation Engineering, Part B: Pavements* **143**(2), 04017006.

ASTM (2012), 'Standard test method for airport pavement condition index surveys'.

Brill, D. and Kawa, I. (2017), Advances in faa pavement thickness design software: Faarfield 1.41, *in* 'Airfield and Highway Pavements 2017', pp. 92–102.

Collop, A. (2000), 'The effect of asphalt layer thickness variations on pavement evaluation using the falling weight deflectometer', *International Journal of Pavement Engineering* **1**(4), 247–263.

Dhakal, N., Elseifi, M. A. and Zhang, Z. (2016), 'Mitigation strategies for reflection cracking in rehabilitated pavements–a synthesis', *International Journal of Pavement Research and Technology* **9**(3), 228–239.

FAA (2006), 'Standardized method of reporting airport pavement strength-pcn, 150/5335-5a', *Advisory Circular, Federal Aviation Administration* .

FAA (2021), 'Airport pavement design and evaluation, ac 150/5320-6g', *Advisory Circular, Federal Aviation Administration* .

Gary, C., Leigh, W. and Michael, H. (2016), 'Airfield pavement design for a major airport using faarfield and apsds'.

Loizos, A., Armeni, A. and Plati, C. (2017), Evaluation of airfield pavements using faarfield, *in* 'Airfield and Highway Pavements 2017', pp. 82–91.

Ma, H. and Zhang, Z. (2020), 'Paving an engineered cementitious composite (ecc) overlay on concrete airfield pavement for reflective cracking resistance', *Construction and Building Materials* **252**, 119048.

Mohammad, L., Elseifi, M., Bae, A., Patel, N., Button, J. and Scherocman, J. (2012), 'Nchrp report 712: optimization of tack coat for hma placement', *Transportation Research Board of the National Academies, Washington, DC* .

O'Massey, R. (1978), 'Aircraft pavement loading: Static and dynamic', *Transportation Research Board Special Report* (175).

Pierce, L. M. and Mahoney, J. P. (1996), 'Asphalt concrete overlay design case studies', *Transportation research record* **1543**(1), 3–9.

Puri, A. (2018), Differentiation of displacement factor for stiff and soft clay in additional modulus of subgrade reaction of nailed-slab pavement system, *in* 'Proceedings of the Second International Conference on the Future of ASEAN (ICoFA) 2017–Volume 2', Springer, pp. 927–933.

Rahman, T., Christady, H., Sartono, W. and Suhendro, B. (2015), Evaluation of bearing capacity and pcn of north runway cakar ayam system in soekarno-hatta international airport using finite element modelling (case study: To operate the b777-300er aircraft).

Rahman, T., Dawson, A. and Thom, N. (2019), The permissible temperature of newly laid asphalt at opening to airfield traffic, *in* 'Bituminous Mixtures and Pavements VII', CRC Press, pp. 365–374.

Rahman, T., Dawson, A., Thom, N., Ahmed, I. and Carvajal-Munoz, J. S. (2020), 'Determining the allowable opening-to-traffic asphalt temperature for airport pavements', *International Journal of Pavement Engineering* pp. 1–19.

Setiawan, D. M. (2020), 'The role of temperature differential and subgrade quality on stress, curling, and deflection behavior of rigid pavement', *Journal of the Mechanical Behavior of Materials* **29**(1), 94–105.

Shahin, M. Y. (2005), *Pavement management for airports, roads, and parking lots*.

Sørensen, A. and Hayven, M. (1982), The dynatest 8000 falling weight deflectometer test system, *in* 'Proceedings of a International Symposium on Bearing Capacity of Roads and Airfields, Volume 1, Trondheim held June 23-25, 1982.'.

Suhendro, B. (2006), 'Sistem cakar ayam modifikasi sebagai alternatif solusi konstruksi jalan di atas tanah lunak'.

Suhendro, B. (2018), Modified chicken claw (cakar ayam modifikasi) system-a new concept in green pavement technology over soft and swampy ground, *in* 'Applied Mechanics and Materials', Vol. 881, Trans Tech Publ, pp. 106–121.

Thom, N. et al. (2013), *Principles of pavement engineering*, Thomas Telford London.

Trevino, M., Dossey, T., McCullough, B. F. and Yildirim, Y. (2003), 'Applicability of asphalt concrete overlays on continuously reinforced concrete pavements', *Center for Transportation Research, University of Texas at Austin* .

Wang, H., Li, M. and Garg, N. (2016), 'Investigation of shear failure in airport asphalt pavements under aircraft ground manoeuvring', *Road Materials and Pavement Design* **18**(6), 1288–1303.

White, G. (2016), 'Shear stresses in an asphalt surface under various aircraft braking conditions', *International Journal of Pavement Research and Technology* **9**(2), 89–101.

Zhao, Z., Guan, X., Xiao, F., Xie, Z., Xia, P. and Zhou, Q. (2020), 'Applications of asphalt concrete overlay on portland cement concrete pavement', *Construction and Building Materials* **264**, 120045.